Crystal field effects on the topological properties of the electron density in molecular crystals: The case of urea

C. Gatti
Centro CNR per lo Studio delle Relazioni tra Struttura e Reattività Chimica, via Golgi 19, I-20133 Milano, Italy

V. R. Saunders
DRAL Daresbury Laboratory, Daresbury, Warrington, Cheshire, WA4 4AD, United Kingdom

C. Roetti
Gruppo di Chimica Teorica, Università di Torino, via Giuria 5, I-10125 Torino, Italy

(Received 25 July 1994; accepted 6 September 1994)

The Quantum Theory of Atoms in Molecules, due to Bader, is applied to periodic systems. Results for molecular and crystalline urea are presented. Changes in both bond critical points and atomic properties due to changes of chemical environment are described. A rationale for the different lengths of the in-plane and out-of-plane hydrogen bonds and for the lengthening of the CO bond in bulk urea is provided in terms of the properties of the Laplacian of the oxygen atom electron density distribution. An evaluation of molecular and atomic volume changes indicates that the decrease of molecular volume upon change of phase from gas to solid originates primarily from a contraction of the atomic basins directly involved in hydrogen bonds. Other atoms show a small expansion. The considerable decrease of oxygen and hydrogen atomic volumes is related to the mutual penetration of their van der Waals envelopes following hydrogen bond formation. The results confirm that urea is more polar in the solid phase. © *1994 American Institute of Physics.*

I. INTRODUCTION

The Quantum Theory of Atoms in Molecules (QTAM) (Ref. 1) has been widely used[2] and, with few exceptions,[3] has received general acceptance. Discussions of its usefulness and validity have appeared.[3,4] The effect of electron correlation on the topology of the electron density has been documented.[5] Among the most recent applications of the QTAM we mention its use to improve the evaluation of magnetic properties,[6] to allow a physically sound interpretation of density current fields,[7] and to develop the chemistry of cohesion and adhesion within and between materials in their bulk state.[8] The QTAM has provided an evaluation of the optimal form factors in x-ray analysis,[9] and topological analysis has been applied[10,11] to experimental electron densities, as derived from x-ray data interpreted within the context of aspherical models.[12] The QTAM permits the investigation of chemical systems on a common basis,[2,8,13] as the theory uses only information contained in the electron density $\rho(\mathbf{r})$. The theory may thus be used for molecules, polymers, surfaces, and solids; the electron density may be described in terms of local (e.g., Gaussian) or nonlocal (e.g., plane wave) basis sets, or even numerically. A unique atomic partitioning of and procedures for a topological analysis of the electron density are defined.

We have developed a computer program to perform the topological analysis of the electron density of a periodic system. In the present work we present a first application of our program to the urea molecular crystal. This system has been investigated,[14] as a test of the possibilities of the *ab initio* Hartree–Fock (HF) fully periodic approach[15] in treating molecular crystals. For hydrogen bonded molecular crystals, such as urea, the main contributions to the intermolecular interaction energy are due to electrostatic interactions, particularly concerning hydrogen bond (HB) formation, and exchange repulsion terms, which are both well accounted for at the HF level. Dispersion forces are expected to provide a minor contribution in the present case. A parallel study of the isolated urea molecule is also presented.

II. COMPUTATIONAL DETAILS

Our implementation of the QTAM (called TOPOND) has been interfaced to CRYSTAL92.[16] The latter is a suite of programs for the calculation of the electronic structure of systems periodic in three (crystals), two (slabs), one (polymer) dimensions and, as a limiting case, molecules, using *ab initio* Hartree–Fock theory and a local (Gaussian) basis. TOPOND has been implemented as one of the options of the CRYSTAL92 properties program. The electron density at a point $\mathbf{r}$ is given by

$$\rho(\mathbf{r}) = \sum_{\mathbf{g},\mathbf{h}} \sum_{i,j} P_{i,j}^{\mathbf{g}-\mathbf{h}} \chi_i^{\mathbf{g}}(\mathbf{r}) \chi_j^{\mathbf{h}}(\mathbf{r}), \tag{1}$$

where $\mathbf{P}$ denotes the one-electron density matrix in the local basis and $\mathbf{g}$ and $\mathbf{h}$ span, in principle, the infinite set of translation vectors.

A. Location of the critical points

The critical points (CP) in the electron density and its Laplacian are the points where $\nabla\rho(\mathbf{r})$ and $\nabla[\nabla^2\rho(\mathbf{r})]$ respectively vanish.[1] In the case of the electron density, given the number of neighbors (NNB) of each of the nonequivalent atoms (NEQA) as a parameter, the program finds the number of unique atom pairs among the NEQA*NNB pairs, which is further reduced to the number of considered pairs using a threshold for the internuclear distance. The search for the

 0021-9606/94/101(12)/10686/11/$6.00

CPs is then performed using the Newton–Raphson algorithm, as in the PROAIMV package,[17,18] starting from the midpoint of the internuclear axis. If no CP is found, the starting point is displaced along the internuclear axis. The displacement in either of the two directions is proportional to the internuclear distance of the atom pair under investigation. In most cases this procedure allows for the automatic recovery of all the bond CPs (BCP) corresponding to both intramolecular and intermolecular interactions. A BCP is such that the density attains its minimum value along the bond path, a line connecting two nuclei where $\rho(\mathbf{r})$ is a maximum with respect to any lateral displacement from the line.[1] BCPs are also denoted $(3,-1)$ CPs, where the first number in parentheses equals the number of nonzero eigenvalues, or principal curvatures, of the Hessian of $\rho(\mathbf{r})$ at the CP, while the second is equal to the sum of the signs of the three eigenvalues. The two negative curvatures are associated with eigenvectors which define an interatomic surface orthogonal to the bond path at the BCP, whereas the positive curvature is associated with an eigenvector defining the bond path at the BCP. Three other kinds of CP, corresponding to local maxima, local minima, and local minima on a surface and maxima in a direction perpendicular to this surface at the CP, can also be recovered by the procedure outlined above. They are referred to as $(3,-3)$, $(3,+3)$, and $(3,+1)$ CP, and are associated with the non-nuclear attractors,[1,19] cages, and rings of the molecular structure,[1] respectively. Quite obviously the $(3,-3)$ critical points associated with each nucleus are not generally recovered by the automatic procedure.

Due to the differing characteristics of the density and Laplacian scalar fields, the procedure for the location of the CPs of the Laplacian is conceptually different. For each of the nonequivalent atoms the Laplacian CPs are sought using a Newton–Raphson algorithm starting from points located on the surface of a sphere, centered on the associated nucleus. The number of starting points is determined by the intervals chosen for the polar coordinates θ and ϕ. By default, the radius is taken to be equal to the distance from the nucleus to the spherical surface where $-\nabla^2\rho(\mathbf{r})$ attains its maximum value in the valence shell of the isolated atom. The choice of different radii permits exploration of other regions of atomic shell concentration or depletion[1] or to take into account the changes in the size of the valence shell charge concentration (VSCC) (Ref. 1) caused by the considerable charge transfer found in some solids, such as ionic crystals.

B. Atomic surfaces and integral properties

Integral properties[1,18] have been computed. The calculation of the properties of atoms in crystals requires a definition of the associated surfaces bounding the atoms. The volume associated with an atom Ω, (the atomic basin), is defined as being enclosed by a surface defined by the boundary condition

$$\nabla\rho(\mathbf{r})\cdot\mathbf{n}(\mathbf{r})=0, \tag{2}$$

where $\mathbf{n}(\mathbf{r})$ is a unit vector normal to the surface at $\mathbf{r}$. The atomic surface is determined indirectly, according to an algorithm proposed by Keith[20] which exploits the following property of the surface: "the finite points of intersection of a given integration ray with the atomic surface satisfy the local condition that the nuclear attractor of the $\nabla\rho(\mathbf{r})$ trajectories intersecting the ray changes, from the nucleus of the atom to another nucleus or vice versa, as the ray passes through these intersections." The time required to determine an atomic surface is then proportional to the number of angular points, and the algorithm turns out to be more costly than that used in PROAIMV.[17] However it overcomes the problem of determining accurately atomic surfaces for atoms bounded by surfaces with many critical points or "near critical" points in the electron density field. These conditions are more commonly the rule than the exception in the case of crystals. Also, in contrast with the molecular case where it is possible to consider all the atoms as possible attractors of a given trajectory, one must define a subset of the atoms of the crystal. Clusters of up to 40 atoms had to be considered in the urea crystal. Given the atomic surface, properties such as atomic moments (including the charge) are evaluated by numerical integration[21] using a coordinate system centered on the nucleus of atom. To reduce the computing time the following techniques have been explored: (i) the generation of an initial guess for the points of intersection of the integration rays with the atomic surface using the intersections obtained with a wave function constructed using a small basis set; (ii) the reduction of the number of angular grid points by using quadrature formulas on the surface of the unit sphere, instead of separate formulas for θ and ϕ;[21] and (iii) the determination of the intersections of a small and uniformly distributed subset of the integration rays as a guess for the starting points of the remaining intersections.[20] More extensive technical details will be published elsewhere. The evaluation of atomic properties is affected by numerical errors which are in our case mainly due to the limited number of angular quadrature points. A compromise between computing time and precision has been adopted and the corresponding results are reported in Table I. Listed under the heading $|L_\Omega|$ are the absolute values of the atomic integrals of the Laplacian (multiplied by 10 000), which should vanish because of the boundary condition imposed on the atomic basins by Eq. (2). The worst case is that of the carbon atom in bulk urea. However the total number of electrons per molecule in bulk urea differs from the theoretical value by less than 0.005. The number of angular points used for the integration of each unique atom, in the bulk and in the gas phase, is also reported in Table I.

C. The derivatives of the electron density

The derivatives of the electron density to second order [for the topological analysis of $\rho(\mathbf{r})$] or up to fourth order [for the topological analysis of $\nabla^2\rho(\mathbf{r})$] are evaluated analytically as follows. The electron density, Eq. (1), may be rewritten[22] as a linear combination of Hermite Gaussian functions (HGF); the latter can be defined as a product of three factors,

$$\Lambda_{ijk}(\alpha,\mathbf{A},\mathbf{r})=\lambda_i(\alpha,A_x,x)\lambda_j(\alpha,A_y,y)\lambda_k(\alpha,A_z,z), \tag{3}$$

where α and $\mathbf{A}$ denote the exponent and centroid, respectively, of the HGF, and

TABLE I. Atomic electron populations, N_Ω, and absolute values of the atomic basin integral of the Laplacian of the charge density multiplied by 10 000, $|L_\Omega|$. NP is the number of angular points used in the determination of the atomic surface.

	OG molecule			CG molecule			Bulk		
Ω	N_Ω	$\|L_\Omega\|$	NP	N_Ω	$\|L_\Omega\|$	NP	N_Ω	$\|L_\Omega\|$	NP
C	3.463	6.3	9 216	3.512	7.2	14 400	3.545	28.4	3 072
O	9.445	1.8	3 072	9.383	1.8	3 072	9.476	3.6	1 536
N	8.468	8.8	14 400	8.481	9.2	14 400	8.568	12.0	3 072
H5	0.521	0.4	3 072	0.508	0.4	3 072	0.454	8.2	768
H7	0.557	0.4	3 072	0.565	0.7	3 072	0.465	9.3	768
Σ_Ω	32.000			32.002			31.995		

$$\lambda_i(\alpha,A_x,x)=(\partial/\partial A_x)^i \exp[-\alpha(x-A_x)^2]. \quad (4)$$

Recursive procedures for the evaluation of the expansion coefficients of the electron density in terms of the HGF are known for Cartesian[23] and spherical harmonic[24] Gaussian basis sets. We note that

$$(\partial/\partial x)^\mu(\partial/\partial y)^\nu(\partial/\partial z)^\tau\Lambda_{ijk}(\alpha,\mathbf{A},\mathbf{r}) = (-1)^{\mu+\nu+\tau}\Lambda_{i+\mu,j+\nu,k+\tau}(\alpha,\mathbf{A},\mathbf{r}). \quad (5)$$

Thus a derivative (of any order) of the electron density with respect to the components of the position vector, $\mathbf{r}$, can be evaluated from values of the HGF (of appropriate order) at that point. The value of a factor of a HGF can be found from the recursion relationship,[23,24]

$$\lambda_{i+1}(\alpha,A_x,x)=2\alpha[(x-A_x)\lambda_i(\alpha,A_x,x) - i\lambda_{i-1}(\alpha,A_x,x)], \quad (6)$$

where it is necessary to adopt the convention that $\lambda_{-1}(\alpha,A_x,x)=0$.

D. Geometry and basis set

Standard[25] molecular basis sets (6-31G**) have been adopted in the present study. The crystal structure of urea (space group $P\bar{4}2_1m$) was taken from a very accurate neutron study,[26] as in previous work.[14] The molecules are linked to each other through HBs between H7 and O atoms (O–H7 length 2.06 Å), to form infinite planar tapes (the atomic numbering scheme for two molecules within a tape is shown in Fig. 1). Adjacent tapes are mutually orthogonal and oriented in opposing directions; their cohesion is provided by the HBs of the H5 atoms with the facing oxygen in the neighboring tape (O–H5 length 1.99 Å). Hence each oxygen is involved in four HBs, two within the tape, and two with neighboring tapes, giving rise to a relatively high experimental sublimation energy [21±0.5 kcal/mol (Ref. 27)]. Computations on the urea molecule at the crystal geometry (CG) and the optimized geometry (OG) within the C_{2v} symmetry constraint were also performed, for the sake of comparison with bulk results.[28] Geometry optimization was performed with GAUSSIAN92 (Ref. 29) using spherical harmonic Gaussian functions, to ensure compatibility with CRYSTAL92.

III. RESULTS AND DISCUSSION

The quality of our basis set and of the corresponding wave function can be inferred from the computed sublimation energy which amounts to 17.4 or 21.8 kcal/mol when OG or CG urea, respectively, are considered as monomers. These results are affected by less than 0.1 kcal/mol by counterpoise estimates[30] of the basis set superposition error.

A. Charge transfer

The formation of HBs in the crystal induces changes in the atomic electron populations, N_Ω, which are the sum of contributions that arise from the change in volume of the atom as the BCPs move (surface term) and changes that take place in the electron distribution within the atomic basin (basin term).[31] All the heavy atoms gain electrons at the expense of the hydrogens in the bulk, see Table I. Following HB formation there is a net flux of 0.067 electrons from the amino-group hydrogen donor to the carbonyl acceptor (the flux is lowered to 0.059 electrons if OG urea is considered). The magnitude and mechanisms of the transfer of charge occurring in the formation of a number of hydrogen bonded complexes have been discussed[32,33] in terms of a generalized Lewis acid and base interaction. Our results can be compared with those for the cyclic formamide dimer (CFD) (Ref. 32) since in this complex both the acidic (N) and the basic atoms

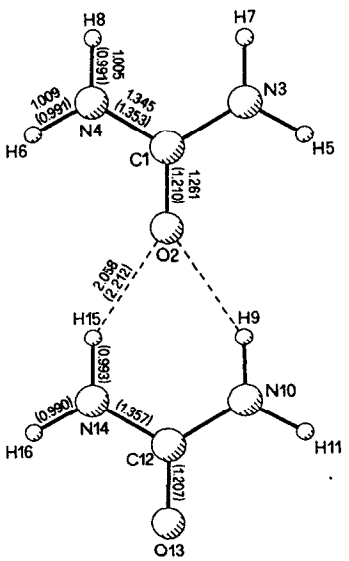

FIG. 1. Atomic numbering scheme for two urea molecules within a crystalline tape. The internuclear distances (Å) refer to the CG with those for the OG in parentheses.

TABLE II. Atomic dipole moments, M_Ω, of molecular and bulk area (atomic units). The component parallel to the C_2 axis (directed from carbon to oxygen) is reported along with the modulus of the dipole moment.

	OG molecule		CG molecule		Bulk	
Ω	M_Ω	$\lvert\mathbf{M}_\Omega\rvert$	M_Ω	$\lvert\mathbf{M}_\Omega\rvert$	M_Ω	$\lvert\mathbf{M}_\Omega\rvert$
C	0.138	0.138	0.056	0.056	0.096	0.096
O	0.688	0.688	0.614	0.614	0.497	0.497
N	−0.149	0.262	−0.162	0.291	−0.141	0.248
H5	−0.079	0.164	−0.073	0.157	−0.066	0.128
H7	0.171	0.171	0.170	0.170	0.136	0.136
Σ_Ω	0.713		0.539		0.451	
M_{CT}	−2.524		−2.559		−3.219	
M_T	−1.811		−2.021		−2.768	

(O) belong to the same molecule (as in urea) and HBs of similar length (1.903 Å in the CFD) are formed. In urea the acidic atom gains three times more electrons than the basic atom (0.100 vs 0.031) if the OG molecule is considered, which agrees qualitatively with that found for the CFD, 0.072 vs 0.029.

The dipole moment, $\mathbf{M}_\Omega$ of an atomic distribution[1,34] is defined by

$$\mathbf{M}_\Omega = -\int_\Omega \rho(\mathbf{r})(\mathbf{r}-\mathbf{r}_\Omega)d\mathbf{r}, \tag{7}$$

where $\mathbf{r}_\Omega$ denotes the position of nucleus of the corresponding atom, the integral being over the atomic basin. The total dipole moment of a neutral fragment is given by[34]

$$\mathbf{M}_T = \sum_\Omega \mathbf{M}_\Omega + \mathbf{M}_{CT} \tag{8}$$

where the charge transfer (CT) contribution, $\mathbf{M}_{CT}$, is

$$\mathbf{M}_{CT} = \sum_\Omega (Z_\Omega - N_\Omega)\mathbf{r}_\Omega, \tag{9}$$

where Z_Ω denotes the nuclear charge. Table II lists the atomic dipole moments for urea in the gas and solid phase. Because of the fields created by CT, the atomic charge distributions become polarized in a direction counter to the direction of CT. Thus in the urea molecule the oxygen atom polarizes towards the positive carbon atom, while the H atoms polarize away from the negative N atom. In the urea molecule the oxygen centroid (computed from $-\mathbf{M}_\Omega/N_\Omega$) is displaced 0.065 a.u. towards C and the H5(H7) centroids 0.308(0.300) a.u. along N–H axes and away from N, these values are lowered to 0.052 and 0.282(0.292) a.u. in the bulk. A slightly greater decrease is found if OG urea is taken as reference. Crystallization is thus accompanied by a reduction in the atomic polarizations. However, the magnitude of the dipole moment is considerably increased in the bulk, because the CT contribution increases its magnitude. The reduction in the atomic polarizations on passing to the bulk serves only to slightly enhance the effect (because the atomic polarization term opposes the CT term).

Listed in Table III are the values Q_Ω of the component of the atomic quadrupole moment for an axis perpendicular to the molecular plane. A negative value for a component implies an accumulation of charge along its associated axis. The reported values indicate that, independent of phase, the electrons preferentially accumulate in a direction perpendicular to the molecular plane. However, following crystallization, both O and N increase their sphericity as a result, for the O atom, of a more uniform concentration in the non bonded regions and, for the N atom, of a transfer of charge from the out-of-plane lone pairs to the C–N bond region.

B. Properties of the BCPs

Parallel to the observed charge migrations, there are interesting changes in the nature of the chemical bonds (Fig. 2 and Table IV), which are discussed first considering CG urea as reference. The BCP displacements are, as expected, lower for ionic interactions (C–O), than for the more covalent ones (C–N,N–H). The latter are characterized by a lower curvature of the electron density (λ_3) parallel with the bond path and the BCP can accordingly be displaced more easily by the perturbation caused by the neighboring urea molecules. This perturbation induces an approximately 40% reduction of the parallel curvature of the C–N bond and a less noticeable increase of the same curvature for the other bonds. The principal curvatures perpendicular to the bond path, λ_1 and λ_2, which are associated with the corresponding eigenvectors of the Hessian of the electron density at the BCP ($\lambda_1 \leqslant \lambda_2 \leqslant \lambda_3$) are affected to a lesser extent by the change of phase and the orientation of the plane of maximum charge accumulation is preserved. This plane is defined by the two eigenvectors corresponding to λ_2 and λ_3 at the BCP and was found to be perpendicular to the molecular plane for all the bonds. The changes in the bond ellipticities ($\epsilon = \lambda_1/\lambda_2 - 1$) and electron density values, ρ_b, at the BCP show the opposite trend with respect to the changes in the parallel curvature, since ϵ and ρ_b increase for the C–N bond on passing from gas to bulk,

TABLE III. Out-of-plane quadrupole moments, Q_Ω, in molecular and bulk area (atomic units).

	OG molecule	CG molecule	Bulk
C	−1.25	−1.18	−1.25
O	−0.45	−0.38	−0.30
N	−2.41	−2.50	−2.14

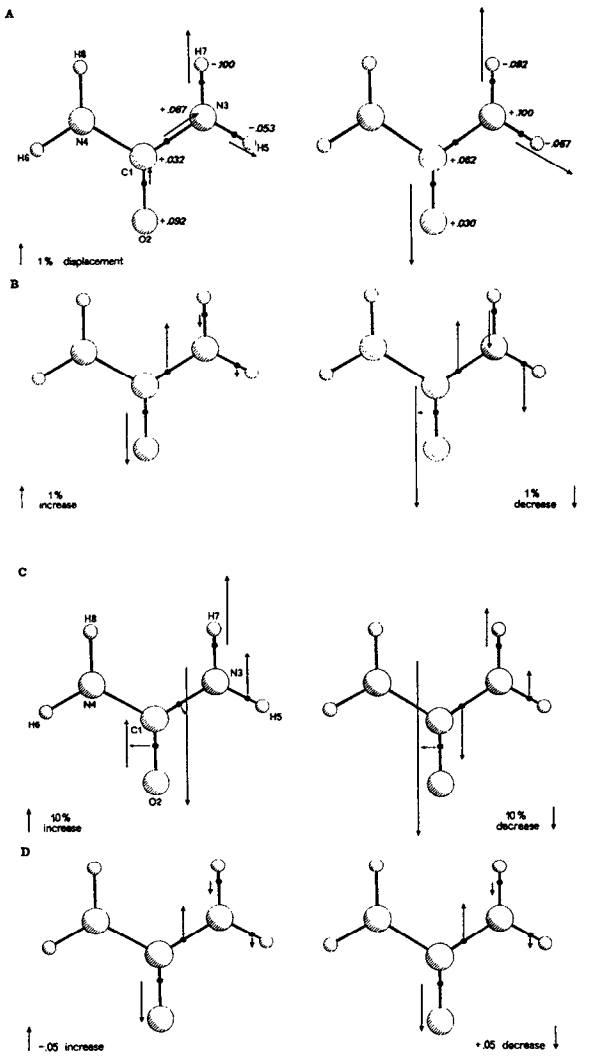

FIG. 2. Changes in the topological properties at BCPs on passing from C_{2v} urea molecule to the bulk (left, crystal geometry; right, RHF/6-31G** optimized geometry). (a) BCP displacements and electron population changes. Arrows are directed according to the observed BCP displacement and their length is proportional to the percentage variation of the BCP distance from the nearest nucleus to the origin of the arrow. Numerical values refer to changes (bulk-molecule) in the atomic basin electron populations (see Table I). (b) Percentage change (bulk-molecule) of the electron density at the BCPs. (c) Percentage change (bulk-molecule) of the parallel curvature of the electron density at the BCPs. (d) Changes in bond ellipticities (bulk-molecule).

while they decrease for all the other bonds. The changes were found to comply with a strengthening and an increased covalent and π character of the C–N bond, whereas the other bonds become more ionic on passing from gas to bulk. The changes are similar to those found comparing CFD vs formamide regarding changes in ρ_b and ϵ of the C–O and of the N–H bonds involved in HBs.[32] However while the C–N bond ellipticity is doubled in bulk urea with respect to the molecule, it decreases in CFD as nitrogen experiences a decrease in its electron population upon dimer formation.

Two different HB CPs are found in the solid as expected on the basis of the urea crystal structure. The topological properties at the HB BCPs are in agreement with the description found for such interactions in gas phase adducts. As anticipated for closed-shell ionic interactions[35] and in accordance with the Pauli principle, charge is removed from the interatomic surface resulting in low ρ_b values, one order of magnitude less than for intramolecular bonds, and positive $\nabla^2\rho_b$ values, with small and nearly equal perpendicular curvatures and a comparatively large parallel curvature. It is interesting to note that the preferred plane of charge accumulation in the molecule (π plane) extends over each infinite planar tape of urea molecules in the bulk. Although the perpendicular curvatures of the HB BCPs within the tape are two order of magnitude smaller than those of intramolecular interactions, their ellipticities are comparable to those of intramolecular interactions. It therefore appears that π-conjugation propagates through HBs. The reliability of our approach in describing HB interactions is testified by the excellent agreement recovered when comparing the experimental topological data of the L-alanine crystal, derived from a 23 K diffraction study[11] with the corresponding periodic Hartree–Fock data.[36] Non-negligible ellipticities for HBs were also found in that case.

The effect of the choice adopted for the gas phase reference geometry on the observed changes in the electron density topological properties upon change of phase are summarized in the following. Figure 2 shows that changes in charge density, parallel curvature, and bond ellipticity values at the BCPs are predicted to be qualitatively similar by both the reference geometries considered. The only exception concerns the parallel curvature of the C–O bond, as a result of its marked dependence on bond length. However the value of the parallel curvature of C–O bond in OG urea, if evaluated at a distance from carbon corresponding to that of BCP in CG urea, amounts to 1.53 a.u., a value which is similar to the value of 1.49 in CG urea and significantly lower than the bulk value of 1.75. Figure 2(a) apparently suggests that some of the BCPs displace in the opposite direction upon change of phase if OG instead of CG urea is taken as reference for the gas phase. This discrepancy is caused by the different bond lengths of the two molecules and is removed when a more careful analysis is made. Indeed, if R_x/R values instead of R_x values, are compared (see Table IV), the same trend for the directions of the BCP displacements are recovered for both reference geometries.

C. Properties of the Laplacian

The topology of the Laplacian field allows one to recover the chemical model of localized bonded and nonbonded pairs and to characterize local concentrations, $\nabla^2\rho<0$, and depletions, $\nabla^2\rho>0$, of the electronic distribution.[35,37] The Laplacian field of an isolated atom reflects the quantum shell structure by exhibiting a corresponding number of alternating shells of charge concentration and charge depletion, beginning with a region of charge concentration at the nucleus. Upon bonding, local maxima and minima are formed in the valence shell of a bonded atom and their number, type, location, and $\nabla^2\rho$ value depend on the linked atom. A local charge concentration is defined by a maximum in $-\nabla^2\rho$, a (3,−3) critical point, whereas a local

TABLE IV. BCPs in molecular and bulk area.

	Bond (x–y)	R (Å)	R_x (Å)	ρ_b	$\nabla^2\rho_b$	λ_1	λ_2	λ_3	ϵ
CG molecule	C–O	1.261	0.415	0.392	−0.55	−1.06	−0.98	1.49	0.074
	C–N	1.345	0.442	0.341	−0.94	−0.85	−0.81	0.73	0.047
	N–H5	1.009	0.775	0.345	−1.92	−1.39	−1.31	0.78	0.059
	N–H7	1.005	0.760	0.351	−1.92	−1.36	−1.28	0.71	0.064
OG molecule	C–O	1.202	0.393	0.432	0.15	−1.27	−1.17	2.59	0.086
	C–N	1.360	0.451	0.332	−0.99	−0.81	−0.77	0.60	0.051
	N–H5	0.991	0.760	0.361	−2.02	−1.47	−1.38	0.83	0.062
	N–H7	0.990	0.751	0.363	−2.01	−1.43	−1.35	0.78	0.065
Bulk	C–O	1.261	0.411	0.381	−0.33	−1.04	−1.04	1.75	0.003
	C–N	1.345	0.451	0.349	−1.15	−0.88	−0.80	0.53	0.099
	N–H5	1.009	0.787	0.344	−1.95	−1.45	−1.38	0.88	0.047
	N–H7	1.005	0.782	0.349	−1.97	−1.45	−1.39	0.87	0.048
	O···H5	1.992	1.293	0.022	0.07	−0.03	−0.03	0.12	0.072
	O···H7	2.058	1.299	0.019	0.07	−0.02	−0.02	0.11	0.036

charge depletion within the VSCC is defined by a (3,+1) or a (3,+3) critical point. It has also been shown[1] that the local charge concentrations and depletions defined in this manner correctly predict the sites of electrophilic and nucleophilic attack, respectively, in a variety of systems.[37] The predictions of structures and geometries of hydrogen-bonded gas phase complexes using the Laplacian of the charge density have been compared[38] with those obtained from a number of other models. The Laplacian predictions were always in good agreement with the *ab initio* and experimental results, even in those cases where other models failed.

Figure 3 displays the location and nature of the Laplacian CPs which are relevant to the discussion of changes occurring upon HB formation. Also reported in the same figure is the numbering (ID) of the different points whose properties are detailed in Tables V and VI. The atomic graphs—the graph denoting the connectivity of the maxima in the VSCC—for a tetrahedral and trigonal carbon atoms were reported in Ref. 39. Carbon in urea possesses three (3,−3) bonded maxima BM in the amide plane, one along each of the C–N bonds (ID 2,2′) and another along the C–O bond (ID 1). Each of the C–N BM is then linked through two (3,−1) saddle points to the BM along the C–O bond (these saddle points are not reported in Fig. 3 and Tables V and VI and lie on either side of the molecular plane). Denoting the BMs as vertices of a triangle, there is a (3,+1) CP (ID 4,4′) in the surface of each ring formed by linking two vertices (ID 2 and 1) and another (3,+1) CP (ID 5,5′) in each of the two surfaces formed by linking three vertices. The latter CPs are the out-of-plane (3,+1) depletions which act as centers of nucleophilic attack at an amide carbon atom. Only the

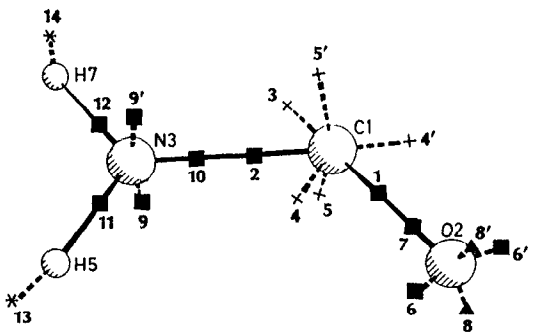

FIG. 3. Location, numbering, and nature of some Laplacian CPs in the VSCC of the amide group atoms, for bulk and gas phase urea. Symbols, ■ (3,−3); ▲ (3,−1); + (3,+1); * (3,+3) CPs.

TABLE V. VSCC Laplacian CPs in molecular urea. ID is the identifying number of the CP (see Fig. 3).

	VSCC	Type	R_x	$-\nabla^2\rho$	ID	Multiplicity
CG molecule	C	(3,−3)	0.954	1.463	1	1
	C	(3,−3)	0.980	1.382	2	2
	C	(3,+1)	0.961	−0.085	3	1
	C	(3,+1)	0.974	−0.164	4	2
	C	(3,+1)	1.079	−0.133	5	2
	O	(3,−3)	0.637	6.051	6	2
	O	(3,−1)	0.731	1.740	7	1
	O	(3,−1)	0.658	3.704	8	2
	N	(3,−3)	0.751	2.276	9	2
	N	(3,−3)	0.816	1.927	10	1
	N	(3,−3)	0.812	2.005	11	1
	N	(3,−3)	0.819	1.900	12	1
	H5	(3,+3)	0.782	−0.165	13	1
	H7	(3,+3)	0.789	−0.163	14	1
OG molecule	C	(3,−3)	0.951	1.645	1	1
	C	(3,−3)	0.983	1.316	2	2
	C	(3,−1)[a]	0.960	−0.069	3	1
	C	(3,+1)	0.977	−0.210	4	2
	C	(3,+1)	1.074	−0.136	5	2
	O	(3,−3)	0.638	5.921	6	2
	O	(3,−3)[b]	0.719	2.291	7	1
	O	(3,−1)	0.656	3.869	8	1[c]
	N	(3,−3)	0.751	2.283	9	2
	N	(3,−3)	0.815	1.887	10	1
	N	(3,−3)	0.814	2.053	11	1
	N	(3,−3)	0.819	1.959	12	1

[a]This is a (3,+1) CP in CG urea.
[b]This is a (3,−1) CP in CG urea.
[c]Two saddle points lying on each side of the molecular plane in CG urea coalesce to one saddle point lying along the C–O axis in OG urea.

TABLE VI. VSCC Laplacian CPs in bulk urea. ID is the identifying number of the CP (see Fig. 3).

VSCC	Type	R_x	$-\nabla^2\rho$	ID	Multiplicity
C	(3,−3)	0.965	1.456	1	1
C	(3,−3)	0.969	1.432	2	2
C	(3,+1)	0.965	−0.128	3	1
C	(3,+1)	0.971	−0.162	4	2
C	(3,+1)	1.090	−0.128	5	2
O	(3,−3)	0.640	5.669	6	2
O	(3,−3)	0.724	1.995	7	1
O	(3,−1)	0.657	3.913	8	2
N	(3,−3)	0.757	2.022	9	2
N	(3,−3)	0.822	1.810	10	1
N	(3,−3)	0.804	2.181	11	1
N	(3,−3)	0.806	2.160	12	1
H5	(3,+3)	0.775	−0.183	13	1
H7	(3,+3)	0.782	−0.181	14	1

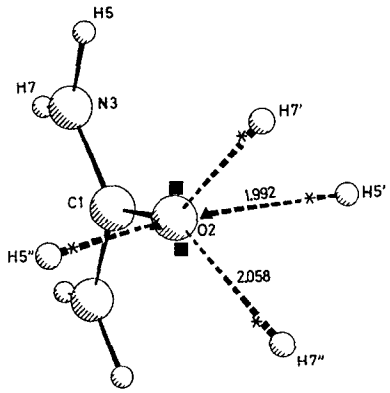

FIG. 4. Hydrogen bonds in bulk urea: the oxygen lone pairs lying in the amide plane, maxima (■) in $-\nabla^2\rho$, are misaligned with the (3,+3) minima (*) of H7′ and H7″ hydrogens. Conversely the saddles (▲) linking lone pairs are perfectly aligned with H5′ and H5″ holes. Hydrogen bonds perpendicular to the molecular plane are therefore stronger and shorter than those in the plane.

(3,−3) CPs in the VSCC of the amide nitrogen atom are reported in Fig. 3 and Tables V and VI. In addition to the in-plane bonded charge concentrations (ID 10-12) the nitrogen has two nonbonded maxima (NBM), one on either side of the molecular plane (ID 9,9′). Besides the single BM (ID 7) along O–C, the keto oxygen possesses two NBMs (ID 6,6′) lying in the amide plane, according to the sp^2 hybridization model. These NBMs are then linked to each other through two saddle points which lie above and below the molecular plane (ID 8,8′). Finally Fig. 3 reports the local charge depletions (ID 13,14) which are found in the nonbonded regions of the hydrogens and which serve as Lewis acids or nucleophilic attack sites for HB formation. These hydrogen charge depletions are characterized by a positive Laplacian and correspond to (3,+3) Laplacian CPs in bulk and CG molecule, and to (3,+1) Laplacian CP in OG molecule.

Tables V and VI show that noticeable changes in the Laplacian values are induced by the change of phase. We consider the keto-oxygen first and try to understand how it can form four HBs in bulk and why the two out-of-plane bonds turn out to be shorter and stronger than the two lying in the molecular plane. Generally the approach of the acidic hydrogen to the base will be such as to align the (3,+3) minimum in the VSCC of the hydrogen with the most suitable (3,−3) base maximum. The oxygen NBMs are the most electron rich region in the base and their negative Laplacian value (6.051 a.u. in CG urea) greatly exceeds the value of the other charge concentrations in the molecule, including those of the competing nitrogen NBMs (2.276 a.u.). The two (3,−1) saddles (ID 8,8′) interconnecting the oxygen NBMs are the second most electron rich regions in the molecule (3.704 a.u.) and they are seen as maxima by hydrogens approaching the oxygen VSCC in a plane which contains the C–O axis and is perpendicular to the molecular plane. HBs can thus be formed either approaching the (3,−3) NBMs or the two saddles interconnecting them. Both options are exploited in bulk urea and each oxygen turns out to be involved in four HBs. Accordingly the two NBMs decrease in value (5.669 a.u.) and the two saddles (ID 8,8′) (3.913 a.u.) increase by a similar amount upon change of phase. The oxygen VSCC changes in such a way as to form a torus of nearly uniform charge concentration in the oxygen nonbonded region. This behavior increases its ability to be involved in more than two HBs. The C–O bond loses some of its π character, a fact suggested also by the decrease of the bond ellipticity and by the decrease of the preferential accumulation of the oxygen charge in a direction perpendicular to the molecular plane (see the discussion on the atomic quadrupole moment components above). Denoting the oxygen NBMs as M and their associated saddles as S, the relative strength of the two kinds of HBs in bulk urea can be appreciated by comparing the angles C–O–M (103.6°) and C–O–S (111.3) with the angles C–O–H7′ (146.6) and C–O–H5′ (106.7), respectively. As shown in Fig. 4 the saddles (▲) are aligned much more efficiently with the H···O axes than are the NBMS (■). Accordingly the HBs involving the saddles are shorter and stronger than those exploiting the NBMs, in spite of the greater $-\nabla^2\rho$ and ρ values at the NBMs. This behavior is rationalized by considering that the saddles are more easily displaced from their molecular location than are the NBMs, since the position of the latter is strongly dependent on oxygen's sp^2 hybridization. In fact the C–O–S angle in CG urea is significantly wider (121.7°) while the C–O–M angle has practically the same width (103.7°) compared to their corresponding values in the bulk. The charge depletion in the hydrogen VSCCs both increase in the bulk and again those associated with the stronger HB are better aligned with respect to the HB axis (Fig. 3) than are the other two. Another point should be mentioned. In OG urea the saddles (ID 8,8′) coalesce to one saddle lying in the molecular plane and this behavior, at variance with the case of CG urea, prevents the oxygen from being involved in more than two HBs. It appears that the lengthening of the C–O bond in bulk urea, with the accompanying loss of π character of the bond and associated changes in the oxygen nonbonded regions, is a fundamental step for the creation of a three-dimensional network of HBs. This may be a quite general mechanism in the formation of hydrogen-bonded

molecular crystals, and is the subject of a current investigation.[40]

The nitrogen VSCC is also considerably affected by HB formation. The two N–H bonded concentrations (ID 11,12) are clearly differentiated in CG urea, the larger being associated with the longer N–H bond involving the hydrogen (H5) syn to the keto-oxygen. When geometrical relaxation is allowed, the two N–H bonds become nearly equal in length (Fig. 1), but the difference in their N–H bonded concentrations is almost entirely preserved in OG urea. Conversely, in bulk urea both charge concentrations increase, since, as a result of an increase of the N–H bond ionicity, they are more tightly bound by nitrogen (compare the changes in the critical point distances R_x in Tables V and VI). The increase for the two charge concentrations is however of a different magnitude, as they become nearly equal in value. The gas-phase asymmetry in the N–H bonded charge concentrations is reduced by the involvement of both kinds of hydrogen in HB interactions. The two NBMs associated with the amide nitrogen lone pair decrease significantly in the bulk, from a $-\nabla^2\rho$ value of 2.276 a.u. in CG urea to 2.022 a.u., owing to the keto-oxygen protonation and the related increase of the C–N π bond character (see the discussion above regarding the increase of ellipticity and the decrease of parallel curvature for this bond).

The (3,+1) out-of-plane charge depletions (ID 5,5′) of the amide carbon VSCC, which are known[1] as the preferred sites of attack by incoming nucleophiles, are not significantly affected by change of phase. They become slightly less charge depleted in the bulk but also more accessible to nucleophiles as their distance from the carbon nucleus increases from 1.079 (CG urea) to 1.090 a.u. The in-plane charge depletion (ID 3), which is associated in the gas phase with the less pronounced hole in the carbon VSCC $-\nabla^2\rho=0.085$ a.u. and which lies opposite the oxygen atom, becomes more charge depleted in the bulk and its $-\nabla^2\rho=0.128$ a.u. equals that of the out-of-plane depletions. Upon change of phase, the latter maintain their role of preferred sites of nucleophilic attack as they still lie significantly further from the carbon nucleus.

The Laplacian distributions of the OG and CG molecules are qualitatively similar, apart from the C–O region where they differ significantly (as was the case for the BCPs). The equalization of the N–H bonded concentrations and the decrease of nitrogen NBMs upon HB formation is a feature common to both reference molecules, notwithstanding the large difference of their N–H bond lengths. On the other hand, it has already been shown how lengthening of the C–O bond with the associated variation of the nonbonded Laplacian distribution for oxygen, permits oxygen participation in more than two HBs.

D. Atomic and functional group volumes

An atomic volume is defined as a region of space enclosed by the intersection of the atomic surface of zero flux and a particular envelope of the electron density.[41] The corresponding functional group or molecular volume is then obtained by summing the volumes of the constituent atoms. Listed under the headings V_1 and V_2 in Table VII are the volumes determined using the 0.001 and the 0.002 a.u. density envelope, respectively. In the case of a solid the atomic basins are obviously finite and the total basin volumes can also be evaluated. They are referred to as V_T in the same table. We consider the comparisons of the molecular volumes first. The computed total molecular volume in the crystal (488.2 a.u.) reproduces quite satisfactorily the volume per molecule in the unit cell (489.5 a.u.) and the difference gives a measure of our volume integration errors. Under a change of phase from gas to solid, a general reduction of volumes is observed. This effect represents the reaction of the molecules to the intermolecular exchange forces. In fact the bulk volume is about 10% less than the gas phase volume if the V_1 values are compared, while the difference reduces to about 2% when the V_2 values are considered. The total molecular volume in bulk, V_T, is very close to V_1 in gas phase (492.1 a.u., CG urea), with gas phase geometry optimization leading these quantities to even better coincidence (488.2 vs 487.3 a.u.). The V_2 values in the gas phase amount on the other hand to only 80% of the bulk V_T value. The ratio of the V_2 and V_1 values is scarcely affected by geometry optimization in the gas phase, while it depends strongly on the phase. V_2 is about 90% and 83% of V_1 in bulk and gas phase, respectively. Again this indicates that the molecular density dies off more rapidly in bulk than in the gas phase. The considerations reported so far do not apply to the individual atomic basins, but they do to the –CO and –NH2 functional groups. This suggests that the two groups behave as the whole molecule upon change of phase, in spite of substantial differential atomic size reorganization within the groups.

The individual atomic volumes are now discussed. In addition to the quantities already introduced, the volume per electron, $W_X=V_X/N_\Omega$ $(X=1,2,T)$, are also listed in Table VII. The carbon in CG urea, being very positively charged (+2.54), is very small in size ($V_1=19.9$ a.u.) and has the lowest volume per electron ($W_1=5.7$). The C atom represents only about 4% of the total molecular volume. Upon change of phase the carbon becomes less positively charged (+2.46) and its V_1 volume increases accordingly, to 21.0 a.u. The V_1 value nearly coincides with V_T for carbon, owing to its high positive charge. The nitrogen atoms undergo an increase of volume upon change of phase and this result holds regardless of the density envelope used. The increase is due mostly to its increased number of electrons, since the volume per electron remains nearly constant as for carbon. In spite of its increased number of electrons, $\Delta N_\Omega=.092$, from CG urea, the keto-oxygen undergoes a marked decrease in volume following HB formation as its V_1 volume in CG urea (132.2 a.u.) is lowered to 115.6 a.u. in bulk. Even V_T (124.3 a.u.) becomes lower than the gas phase V_1 value. An inspection of the volume per electron values reveals that considerable charge contraction occurs in the oxygen basin, more than that of the molecule as a whole (86% vs 91% if CG urea is taken as reference and the W_1 values are used). The largest decrease occurs however with the hydrogens. Upon HB formation, their V_1 and V_2 volumes are lowered to less than 70% and about 80%, respectively, of the corresponding gas phase values. The volume decrease of the hydrogens is not only due to their loss of electrons (Fig. 2 and Table I) but

TABLE VII. Volume (a.u.) V_X ($X=1, 2, T$)[a] and volume/electron $W_X = V_X/N_\Omega$ for atoms and functional groups in molecular and bulk urea. The experimental molecular volume in the bulk is 489.5 a.u.

	Ω	V_1	V_2	V_T	W_1	W_2	W_T
CG molecule	C	19.9	18.5		5.7	5.3	
	O	132.2	111.1		14.1	11.8	
	N	117.9	101.4		13.9	12.0	
	H5	24.6	18.8		48.6	37.0	
	H7	27.4	20.8		48.5	36.8	
	CO	152.1	129.6		11.8	10.1	
	NH_2	170.0	140.9		17.8	14.8	
	molecule	492.1	411.5		15.4	12.9	
OG molecule	C	18.7	17.4		5.4	5.0	
	O	129.7	108.9		13.7	11.5	
	N	118.0	100.8		13.9	11.9	
	H5	24.7	18.9		47.4	36.3	
	H7	26.7	20.2		47.9	36.2	
	CO	148.4	126.3		11.5	9.8	
	NH_2	169.4	139.8		17.7	14.6	
	molecule	487.3	406.0		15.2	12.7	
Bulk	C	21.0	19.1	21.2	5.9	5.4	6.0
	O	115.6	104.6	124.3	12.2	11.0	13.1
	N	120.2	107.5	135.0	14.0	12.6	15.8
	H5	16.8	15.3	17.7	37.0	33.6	39.0
	H7	18.2	16.3	18.7	39.1	35.0	40.1
	CO	136.6	123.7	145.5	10.5	9.5	11.2
	NH_2	155.2	139.1	171.4	16.4	14.7	18.1
	molecule	447.0	401.8	488.2	14.0	12.6	15.3

[a] V_1 and V_2 refer to the volume of the atomic (or group) basin where the electronic charge exceeds 0.001 or 0.002 a.u., respectively. V_T is the volume of the atomic basin defined by the surface given by Eq. (2), and is finite only for solid systems.

also to their 30% increase in average density. The decrease of the size of hydrogens involved in HBs is a well known[42] from experiment, since the contact distance of the donor and acceptor atom in hydrogen bonded molecular crystals is practically identical to the sum of the van der Waals radii of acceptor and donor. A conclusion which is often drawn[42] is that the van der Waals radius of the interleaving H atom is almost zero. It has been shown that upon formation of an intermolecular HB, the van der Waals envelopes of the hydrogen and base penetrate each other with an associated decrease in the volume of the complex with respect to the sum of the individual partners' volumes.[33,38,41] They also demonstrate[33] that the strength of the hydrogen bond correlates with the degree of interpenetration of the two van der Waals envelopes. As a measure of the extent of penetration they considered Δr, the difference between the non bonded radius of the hydrogen or of the base in the isolated molecule and the distance from the corresponding atoms to the HB CP (R_X, Table IV). The nonbonded radius was defined as the average distance from the nucleus to the 0.001 a.u. contour, the nonbonded radii of hydrogens and oxygen in gas phase urea being 2.02 and 3.00 a.u. The corresponding Δr values are equal to 0.70 and 0.56 a.u. for the shorter HB and to 0.59 and 0.54 for the longer HB. As expected, the highest Δr values correspond to the shorter and stronger of the two kind of HB and their bond length difference results mostly from H5 being penetrated much more efficiently than H7. The total interpenetration of the two van der Waals envelopes amounts, respectively, to 1.26 and to 1.14 a.u. The contraction of molecular volume upon change of phase from gas to solid is not the result of a general contraction of the individual atoms forming the molecule but originates from the dominance of the large contraction of the atomic basins directly involved in the HBs, with hydrogens contributing the most, over the small expansion of the remaining basins. The hydrogens in bulk urea maintain a non-negligible van der Waals radius, at variance with common thinking. This result is possible for the associated nearly equal decrease of the oxygen radius (at least for the longer HB).

It has been shown[41] that V_1 yields molecular sizes that are in agreement with those determined from the analysis of kinetic theory data for gas phase molecules, whereas V_2 yields molecular sizes that can be employed in describing the closer packing found in the solid state.[41,43] For example, the molecular shape determined by the 0.002 a.u. contour has been used[44] to rationalize the observed packing of O_2 molecules in the α phase of the solid.

Figure 5 displays $\nabla\rho$ trajectories (right) and electron density contour plots (left) in the molecular plane of OG urea (top) and bulk urea (bottom). The contour plots are overlaid with the two $\nabla\rho$ trajectories which originate at each BCP. These trajectories define the molecular structure (molecular graph). The molecular graph for bulk urea demonstrate that each oxygen atom is involved in four HBs, two within the tape (see Fig. 1), and two with neighboring tapes. Figure 5 also confirms the considerable decrease of the hydrogen atomic volumes accompanying crystallization.

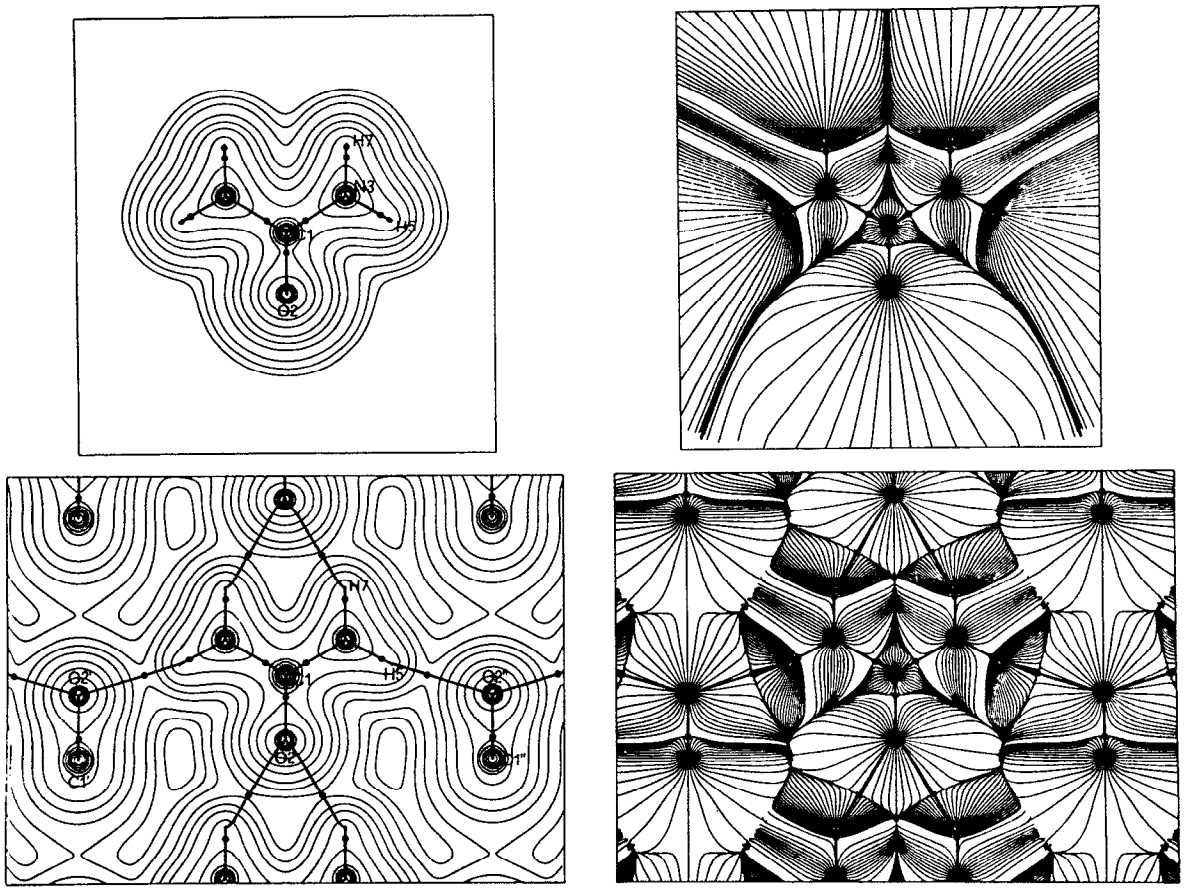

FIG. 5. $\nabla\rho$ trajectories (right) and electron density contour plots (left) in the molecular plane of OG urea (top) and bulk urea (bottom). The contour plots are overlaid with the two $\nabla\rho$ trajectories which originate at each BCP (●).

IV. CONCLUSIONS

The present work shows that upon change of phase from gas to solid, organic molecules undergo easily rationalizable variations in their atomic properties and in their electron density and Laplacian CP characteristics. The changes in topological and atomic properties with change of phase in urea are small. However they are greater (by more than one order of magnitude) than those typically found when comparing the properties of a given functional group or of a repeating unit in a series of different molecules.[39] A rationale for the different lengths of the in-plane and out-of-plane HBs and for the associated lengthening of CO bond in bulk urea has been provided. Atomic volume changes have been evaluated; contraction of the oxygen and hydrogen atomic volumes has been related to mutual penetration of their van der Waals envelopes upon HB formation.

In previous work on urea[14] the effects of change of phase were discussed in terms of band structure, density of states (DOS) and charge difference maps. Some bands were rather flat, corresponding to molecular states only slightly perturbed by the crystalline environment. Other bands, and in particular those involving hydrogen atoms, exhibit considerable dispersion. The present results confirm that the solid state effects induce the greatest changes in the hydrogen charge distribution. However, we find variations in the oxygen and nitrogen VSCCs as well. Actually, a careful inspection of the DOS profiles[14] shows that nitrogen and oxygen atoms also contribute significantly to the bands exhibiting the largest dispersion. The present analysis agrees with the conclusion based on electron density difference maps[14] that the crystalline environment favors more ionic charge distributions, the molecular dipole moment being found to be much larger in the bulk, the magnitude of all atomic net charges apart from carbon increasing. The C–N bond becomes more covalent, the remainder more ionic.

The present study, though restricted to one system, suggests that the QTAM is a very useful theoretical tool for the investigation of the nature of chemical interactions in periodic systems, enhancing our understanding of crystal field effects.

ACKNOWLEDGMENTS

The present work has been supported by the Human Capital and Mobility programme of the European Community under Contract No. CHRX-CT93-0155. The help of Mr. M. Bandera in preparing the drawings is gratefully acknowledged.

[1] R. F. W. Bader, in *Atoms in Molecules: A Quantum Theory*, International Series of Monographs on Chemistry 22 (Oxford University, Oxford, 1990).

[2] R. F. W. Bader, Chem. Rev. **91**, 893 (1991).
[3] C. L. Perrin, J. Am. Chem. Soc. **113**, 2865 (1991).
[4] C. Gatti and P. Fantucci, J. Phys. Chem. **97**, 11 677 (1993).
[5] C. Gatti, P. J. MacDougall, and R. F. W. Bader, J. Chem. Phys. **88**, 3792 (1988).
[6] T. A. Keith and R. F. W. Bader, Chem. Phys. Lett. **194**, 1 (1992); **210**, 223 (1993).
[7] T. A. Keith and R. F. W. Bader, J. Chem. Phys. **99**, 3669 (1993); R. F. W. Bader and T. A. Keith, *ibid.* **99**, 3683 (1993).
[8] M. E. Eberhart, M. M. Donovan, J. M. Maclaren, and D. P. Clougherty, Prog. Surf. Sci. **36**, 1 (1991).
[9] P. F. Zou and R. F. W. Bader, Acta Crystallogr. (submitted).
[10] M. Kappkhan, V. G. Tsirel'son, and R. P. Ozerov, Dokl. Akad. Nauk SSSR **303**, 404 (1988); S. T. Howard, M. B. Hursthouse, C. W. Lehmann, P. R. Mallinson, and C. S. Frampton, J. Chem. Phys. **97**, 5616 (1992); W. T. Kloster, S. Swaminathan, R. Nanni, and B. M. Craven, Acta Crystallogr. B **48**, 217 (1992).
[11] R. Destro, R. Bianchi, C. Gatti, and F. Merati, Chem. Phys. Lett. **186**, 47 (1991); C. Gatti, R. Bianchi, R. Destro, and F. Merati, J. Mol. Struct. (THEOCHEM) **255**, 409 (1992).
[12] R. F. Stewart, Acta Crystallogr. A **32**, 565 (1976).
[13] C. Gatti, in *Clusters Models for Surface and Bulk Phenomena*, edited by P. Bagus and G. Pacchioni (Plenum, New York, 1992), p. 651.
[14] R. Dovesi, M. Causà, R. Orlando, C. Roetti, and V. R. Saunders, J. Chem. Phys. **92**, 7402 (1990).
[15] C. Pisani, R. Dovesi, and C. Roetti, *Hartree–Fock Ab Initio Treatment of Crystalline Systems*, Lecture Notes in Chemistry 48 (Springer, Berlin, 1988).
[16] R. Dovesi, V. R. Saunders, and C. Roetti, CRYSTAL92-*An ab initio Hartree–Fock LCAO program for periodic systems-User Manual*, 1992.
[17] PROAIMV, McMaster University, Ontario, Canada, 1992.
[18] F. W. Biegler-König, R. F. W. Bader, and T. Tang, J. Comput. Chem. **3**, 317 (1982).
[19] C. Gatti, P. Fantucci, and G. Pacchioni, Theor. Chim. Acta **72**, 433 (1987); W. L. Cao, C. Gatti, P. J. MacDougall, and R. F. W. Bader, Chem. Phys. Lett. **141**, 380 (1987); J. Cioslowski, J. Phys. Chem. **94**, 5496 (1990); G. I. Bersuker, C. Peng, and J. E. Boggs, J. Phys. Chem. **97**, 9323 (1993); C. Mei, K. E. Edgecombe, V. H. Smith Jr., and A. Heilingbrunner, Int. J. Quantum Chem. **48**, 287 (1993).
[20] T. A. Keith, Ph.D. thesis, McMaster University, 1993.
[21] A. H. Stroud, *Approximate Calculations of Multiple Integrals* (Prentice–Hall, Englewood Cliffs, 1971).
[22] V. R. Saunders, C. Freyria-Fava, R. Dovesi, L. Salasco, and C. Roetti, Mol. Phys. **77**, 629 (1992).
[23] L. E. McMurchie and E. R. Davidson, J. Comp. Phys. **26**, 218 (1978).
[24] V. R. Saunders, in *Methods in Computational Molecular Physics*, edited by G. H. F. Diercksen and S. Wilson (Reidel, New York, 1984), p. 1.
[25] W. J. Hehre, L. Radom, P. v. R. Schleyer, and J. A. Pople, *Ab initio Molecular Orbital Theory* (Wiley, New York, 1986).
[26] S. Swaminathan, B. M. Craven, and R. K. McMullan, Acta Crystallogr. B **40**, 300 (1984).
[27] K. Suzuki, S. Onishi, T. Koide, and S. Seki, Bull. Chem. Soc. Jpn. **29**, 127 (1956).
[28] A C_2 form of the isolated urea molecule is however slightly lower in energy (−1.13 and −1.99 kcal/mol at the 6-31G** and MP2/6-31G** levels, respectively) than the C_{2v} form.
[29] GAUSSIAN92, Revision B, M. J. Frisch, G. W. Trucks, M. Head-Gordon, P. M. W. Gill, M. W. Wong, J. B. Foresman, B. G. Johnson, H. B. Schlegel, M. A. Robb, E. S. Replogle, R. Gomperts, J. L. Andres, K. Raghavachari, J. S. Binkley, C. Gonzalez, R. L. Martin, D. J. Fox, D. J. Defrees, J. Baker, J. J. P. Stewart, J. A. Pople, Gaussian Inc., Pittsburgh, Pennsylvania, 1992.
[30] S. F. Boys and F. Bernardi, Mol. Phys. **19**, 553 (1970).
[31] T. S. Slee, J. Am. Chem. Soc. **108**, 7541 (1986).
[32] J. R. Cheeseman, M. T. Carroll, and R. F. W. Bader, Chem. Phys. Lett. **143**, 450 (1988).
[33] M. T. Carroll and R. F. W. Bader, Mol. Phys. **65**, 695 (1988).
[34] R. F. W. Bader, A. Larouche, C. Gatti, M. T. Carroll, P. J. MacDougall, and K. B. Wiberg, J. Chem. Phys. **87**, 1142 (1987).
[35] R. F. W. Bader and H. J. Essen, Chem. Phys. **80**, 1943 (1984).
[36] C. Gatti, in Proceedings of QUITEL XX, Merida, Venezuela, October, 1992 (unpublished).
[37] R. F. W. Bader, P. J. MacDougall, and C. D. H. Lau, J. Am. Chem. Soc. **106**, 1594 (1984).
[38] M. T. Carroll, C. Chang, and R. F. W. Bader, Mol. Phys. **63**, 387 (1988).
[39] R. F. W. Bader, P. L. A. Popelier, and C. Chang, J. Mol. Struct. (THEOCHEM) **255**, 145 (1992).
[40] C. Gatti, F. Cargnoni, and R. Destro (in preparation).
[41] R. F. W. Bader, M. T. Carroll, J. R. Cheeseman, and C. Chang, J. Am. Chem. Soc. **109**, 7968 (1987).
[42] G. Gilli, in *Fundamentals of Crystallography*, IUC Texts on Crystallography 2, edited by C. Giacovazzo (Oxford University, Oxford, 1992), p. 465.
[43] R. F. W. Bader and H. J. T. Preston, Theor. Chim. Acta **17**, 384 (1970).
[44] C. S. Barrett and L. Meyer, Phys. Rev. **160**, 694 (1967).